Suppression of ferromagnetism and influence of disorder in silicon-substituted $CeRh_6Ge_4$

Y. J. Zhang,[1,2,3] Z. Y. Nie,[2] R. Li,[2] Y. C. Li,[4] D. L. Yang,[4] B. Shen,[2] Y. Chen,[2] F. Du,[2] S. S. Luo,[2] H. Su,[2] R. Shi,[1] S. Y. Wang,[1] M. Nicklas,[5] F. Steglich,[2,5] M. Smidman,[2,3,*] and H. Q. Yuan[2,3,6,7,†]

[1]*Institute for Advanced Materials, Hubei Normal University, Huangshi 435002, China*

[2]*Center for Correlated Matter and Department of Physics, Zhejiang University, Hangzhou 310058, China*

[3]*Zhejiang Province Key Laboratory of Quantum Technology and Device, Department of Physics, Zhejiang University, Hangzhou 310058, China*

[4]*Beijing Synchrotron Radiation Facility, Institute of High Energy Physics, Chinese Academy of Sciences, Beijing 100049, China*

[5]*Max Planck Institute for Chemical Physics of Solids, Dresden, Germany*

[6]*State Key Laboratory of Silicon Materials, Zhejiang University, Hangzhou 310058, China*

[7]*Collaborative Innovation Center of Advanced Microstructures, Nanjing 210093, China*

(Received 24 March 2022; revised 30 June 2022; accepted 25 July 2022; published 8 August 2022)

We report a study of isoelectronic chemical substitution in the recently discovered quantum critical ferromagnet $CeRh_6Ge_4$. Upon silicon doping, the ferromagnetic ordering temperature of $CeRh_6(Ge_{1-x}Si_x)_4$ is continuously suppressed, and no transition is observed beyond $x_c \approx 0.125$. Non-Fermi-liquid behavior with $C/T \propto \ln(T^*/T)$ is observed close to x_c, indicating the existence of strong quantum fluctuations, while the T-linear behavior observed upon pressurizing the parent compound is absent in the resistivity, which is likely a consequence of the disorder induced by silicon doping. Our findings show the effects of disorder on the unusual ferromagnetic quantum criticality in $CeRh_6Ge_4$, and provide further evidence for understanding the origin of this behavior.

DOI: 10.1103/PhysRevB.106.054409

I. INTRODUCTION

Quantum critical points (QCPs) are of extensive interest for understanding the physics of correlated electron systems, owing to the emergence of exotic quantum phenomena such as unconventional superconductivity and non-Fermi-liquid behavior [1,2]. Heavy-fermion metals are ideal systems for examining quantum criticality since nonthermal parameters such as pressure, chemical doping, or magnetic fields can effectively tune the relative strengths of the Ruderman-Kittel-Kasuya-Yosida interaction and the Kondo interaction, leading to the continuous suppression of a second-order phase transition to a QCP [3–7].

QCPs have been extensively observed in antiferromagnetic systems [8–11], but are rarely found in ferromagnetic (FM) materials, where the FM transition usually vanishes suddenly or converts to antiferromagnetic order upon increasing the tuning parameter [12]. Recently, the stoichiometric heavy-fermion compound $CeRh_6Ge_4$ was found to exhibit a FM QCP upon tuning with hydrostatic pressure [13,14]. Its ferromagnetic transition is continuously suppressed to zero at $p_c \approx 0.8$ GPa, where there is also strange metal behavior with a linear temperature dependence of the resistivity and a logarithmic divergence of the specific-heat coefficient [13]. These findings are in contrast to the anticipated absence of FM QCPs in clean itinerant ferromagnetic systems [15,16], and a local QCP scenario with localized ferromagnetism and magnetic anisotropy has been proposed to resolve this contradiction [13]. A localized nature of the $4f$ electrons in $CeRh_6Ge_4$ was revealed in the subsequent study of quantum oscillations and density functional theory calculations [17]. Meanwhile, angle-resolved photoemission spectroscopy [18], ultrafast optical spectroscopy [19], and inelastic neutron scattering [20] provide evidence for anisotropic hybridization between the conduction and $4f$ electrons in $CeRh_6Ge_4$.

The application of hydrostatic pressure to stoichiometric $CeRh_6Ge_4$ was vital for revealing the existence of a FM QCP without the introduction of disorder, which is inherently present upon chemical doping. However, some experimental methods including thermal expansion and inelastic neutron scattering are extremely limited under pressure, which are essential for characterizing the QCP, such as the analysis of the divergent behavior of the Grüneisen ratio [9,21,22] and searching for E/T scaling in the dynamic susceptibility [23]. Achieving a FM QCP via chemical substitution would expand the range of techniques which could be applied to probe the ferromagnetic quantum criticality in $CeRh_6Ge_4$.

Moreover, the investigation of chemical substitution in $CeRh_6Ge_4$ allows for an examination of the influence of disorder on the quantum critical behaviors in the vicinity of a FM QCP. In the aforementioned framework for clean itinerant ferromagnetic systems [15,16], the transition is predicted to become first order below a temperature T_{tc}. The introduction of disorder suppresses T_{tc} until it disappears above a critical disorder strength [24], and the resulting continuous quantum phase transition may be accompanied by phenomena such as quantum Griffiths or Kondo cluster-glass phases [25–27]. On the other hand, given that $CeRh_6Ge_4$ is a clean stoichiometric

*msmidman@zju.edu.cn
†hqyuan@zju.edu.cn

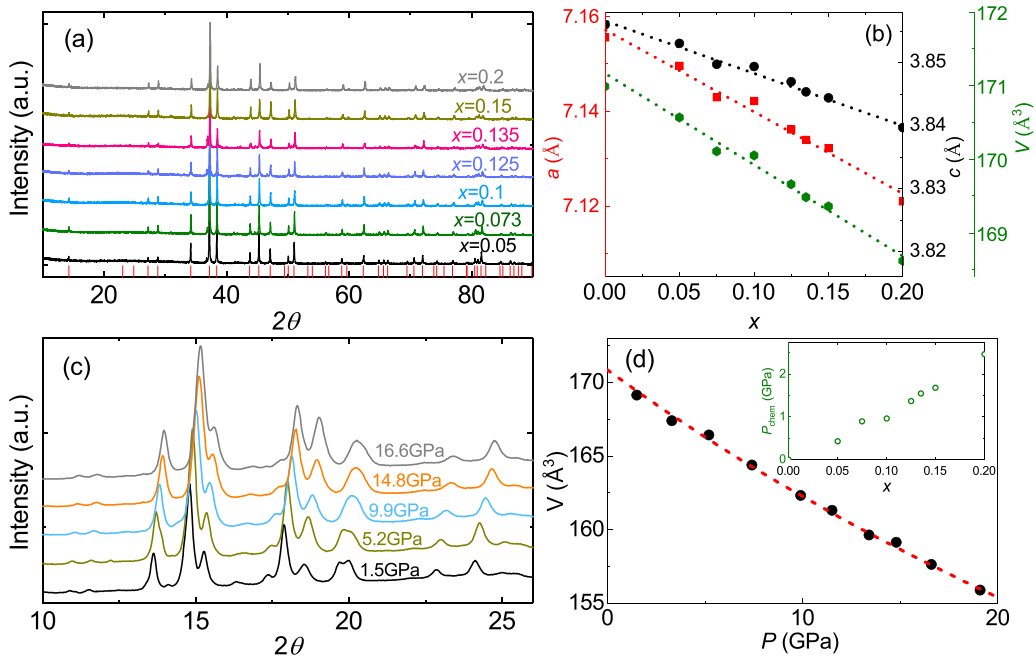

FIG. 1. (a) X-ray diffraction (XRD) patterns of powdered $CeRh_6(Ge_{1-x}Si_x)_4$ polycrystalline samples measured at room temperature, where the positions of the Bragg peaks corresponding to $CeRh_6Ge_4$ are marked by red vertical lines. (b) The lattice constants a, c and the unit-cell volume V as a function of x for $CeRh_6(Ge_{1-x}Si_x)_4$. Data for a, c, and V are represented by red squares, black circles, and olive hexagons, respectively, and the dashed lines are guides to the eye. (c) High-pressure XRD patterns of $CeRh_6Ge_4$, measured with a monochromatic beam of wavelength 0.6199 Å at room temperature. (d) Unit-cell volume of $CeRh_6Ge_4$ as a function of pressure, obtained from refining the high-pressure powder XRD results. The dashed line represents the results from fitting with Eq. (1). The inset shows the x dependence of the chemical pressure P_{chem}.

system where a FM QCP can already be induced by hydrostatic pressure [13], it is of particular interest to examine the effects of disorder on this very different class of quantum critical ferromagnetic materials.

Here, in order to scrutinize these problems, we successfully synthesized a series of silicon-substituted $CeRh_6Ge_4$ samples. Their structural and physical properties are investigated using x-ray diffraction, magnetization, electrical resistivity, and specific-heat measurements. The reduction of the unit-cell volume with increasing silicon concentration demonstrates that chemical pressure has been applied relative to $CeRh_6Ge_4$. The $T-x$ phase diagram is constructed for $CeRh_6(Ge_{1-x}Si_x)_4$, where T_C is completely suppressed upon silicon doping at around $x_c \approx 0.125$. The logarithmic divergence of C/T observed close to x_c indicates the existence of strong quantum fluctuations in silicon-doped $CeRh_6Ge_4$, but the T-linear temperature dependence of the resistivity observed for the stoichiometric compound [13] is found to be absent in the resistivity, likely due to the influence of disorder.

II. EXPERIMENTAL DETAILS

Polycrystalline samples of $CeRh_6(Ge_{1-x}Si_x)_4$ were synthesized by arc melting in a titanium-gettered argon atmosphere, with a stoichiometric composition of Ce ingot (99.9%), Rh ingot (99.95%), and $Ge_{1-x}Si_x$ ingot [28]. The precursor $Ge_{1-x}Si_x$ ingots were prepared by alloying Ge ingot (99.999%) with Si ingot (99.999%) in the nominal atomic ratio. The obtained $CeRh_6(Ge_{1-x}Si_x)_4$ ingots were wrapped in Ta foil and sealed in evacuated quartz tubes before being annealed at 1100 °C for one week, and then cooled slowly to 600 °C. The composition of all doped samples was determined by energy-dispersive x-ray spectroscopy (EDX). Here we use the nominal values for the Si composition x, which agree well with those found from EDX measurements. The crystal structure was characterized at room temperature using powder x-ray diffraction, and the high-pressure x-ray diffraction measurements of stoichiometric $CeRh_6Ge_4$ at room temperature were performed at the 4W2 beamline at the Beijing Synchrotron Radiation Facility (BSRF) with a monochromatic beam of wavelength 0.6199 Å. The heat capacity was measured down to 0.4 K using a Quantum Design Physical Property Measurement System (PPMS) with a ^{3}He insert. The resistivity was measured down to 1.8 and 0.4 K in a PPMS and ^{3}He refrigerator, respectively. Magnetization measurements were performed down to 0.5 K using a Magnetic Property Measurement System with a ^{3}He insert.

III. RESULTS

Powder XRD patterns for $CeRh_6(Ge_{1-x}Si_x)_4$ are shown in Fig. 1(a), where the peak positions can be well indexed on the basis of the hexagonal $CeRh_6Ge_4$ structure. In order to reveal the evolution of the lattice with silicon substitution, the refined lattice constants $a(x)$, $c(x)$, and unit-cell volume $V(x)$ are displayed in Fig. 1(b). Up to $x = 0.2$, all the lattice constants a, c and unit-cell volume V decrease linearly as a function of x, which is due to the isoelectronic substitution of the larger germanium atom with the smaller silicon. The a/c ratio is almost independent of x, with a $a/c = 1.85$, which

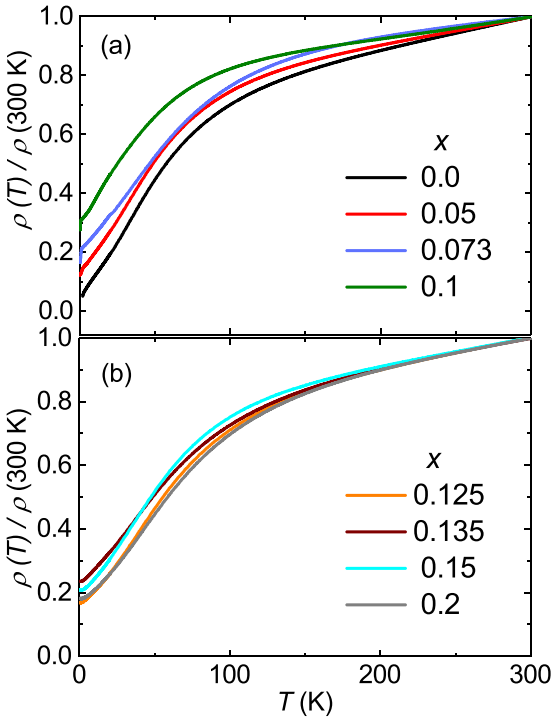

FIG. 2. Temperature dependence of the normalized resistivity $\rho(T)/\rho(300\ \mathrm{K})$ for samples with doping concentrations (a) $x \leqslant 0.1$ and (b) $x \geqslant 0.125$.

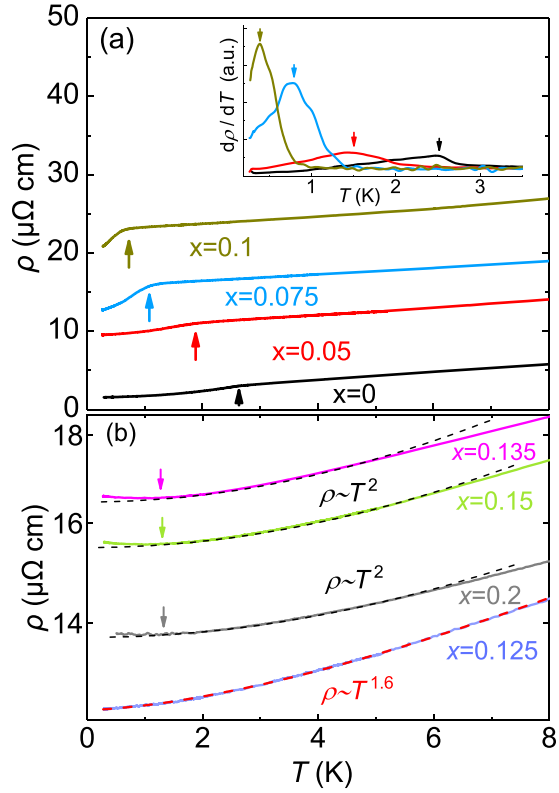

FIG. 3. (a) Low-temperature resistivity $\rho(T)$ for $x \leqslant 0.1$. The inset shows the derivative $d\rho/dT$ for $x \leqslant 0.1$. The arrows correspond to the ferromagnetic transition at T_C. (b) Low-temperature resistivity $\rho(T)$ for $x \geqslant 0.125$. The red dashed line shows a fit to non-Fermi-liquid behavior with $\rho(T) \sim T^{1.6}$, the arrows mark the upturn behavior at low temperature, and the black dashed lines correspond to Fermi-liquid behavior from which the low-temperature data deviate.

is similar to that reported for $CeRh_6Ge_4$ single crystals [29]. The continuous lattice contraction and constant value of a/c indicate the absence of a change in the crystal structure of $CeRh_6(Ge_{1-x}Si_x)_4$.

In order to reveal the pressure evolution of the lattice constants in $CeRh_6Ge_4$ and to estimate the equivalent chemical pressure induced by Si/Ge substitution, high-pressure XRD measurements of $CeRh_6Ge_4$ were conducted in the pressure range 1.5 to 16.6 GPa, and the high-pressure XRD patterns are displayed in Fig. 1(c). The obtained volume V as a function of pressure is displayed in Fig. 1(d), where the volume continuously decreases upon applying pressure, indicating the absence of a pressure-induced structural transition in $CeRh_6Ge_4$. The data are well fitted by [30]

$$P_{\mathrm{chem}} = \frac{3B_0}{2}\left[\left(\frac{V_0}{V}\right)^{\frac{7}{3}} - \left(\frac{V_0}{V}\right)^{\frac{5}{3}}\right], \qquad (1)$$

giving rise to a bulk modulus $B_0 = 174(3)$ GPa and zero pressure volume $V_0 = 170.9(2)$ Å^3. The isoelectronic substitution of silicon for germanium has a similar effect to hydrostatic pressure, both resulting in a contraction of the lattice. In order to reveal the chemical pressure of silicon doping, P_{chem} as function of x is shown in the inset, where P_{chem} is estimated from comparing the values of the lattice volume under silicon doping and pressure.

The temperature dependence of the normalized resistivity $\rho(T)/\rho(300\ \mathrm{K})$ for $CeRh_6(Ge_{1-x}Si_x)_4$ is shown in Figs. 2(a) and 2(b). It is clear that the residual resistivity ratio RRR decreases with doping for $x \leqslant 0.1$, while the RRR are almost constant or slightly increase from $x = 0.135$ to 0.2. The latter likely corresponds to competition between the effects of increased disorder which enhances the residual resistivity, and the reduction of critical fluctuations upon moving away from the critical concentration [13].

Figure 3 displays the resistivity $\rho(T)$ and corresponding derivatives $d\rho/dT$ at temperatures below 8 K for various x. As seen in Fig. 3(a), both $\rho(T)$ and $d\rho/dT$ for $x = 0$ show an anomaly at T_C, which corresponds to the ferromagnetic ordering transition reported previously [13,28]. With increasing x, the transition is suppressed to lower temperatures, and disappears beyond $x = 0.1$. For $x = 0.125$, no transition is observed in $\rho(T)$ down to the lowest measured temperature, and there is non-Fermi-liquid behavior. The non-Fermi-liquid behavior was analyzed using the expression $\rho \sim T^{1.6}$, as shown in Fig. 3(b), which is different from the T-linear behavior observed at the FM QCP in stoichiometric $CeRh_6Ge_4$ [13]. For $x \geqslant 0.135$, with decreasing temperature below 1.0 K, there is a weak upturn of $\rho(T)$, as marked by the arrows in Fig. 3(b). These upturn behaviors may be a consequence of the enhanced disorder induced by silicon doping. On the other hand, above the temperature of the resistivity minimum T_{min}, the behavior can be well analyzed using the Fermi-liquid expression $\rho \sim T^2$, as shown by the dashed lines.

The low-temperature C/T is displayed in Fig. 4. For $x \leqslant 0.1$, a sharp transition is observed in C/T, corresponding

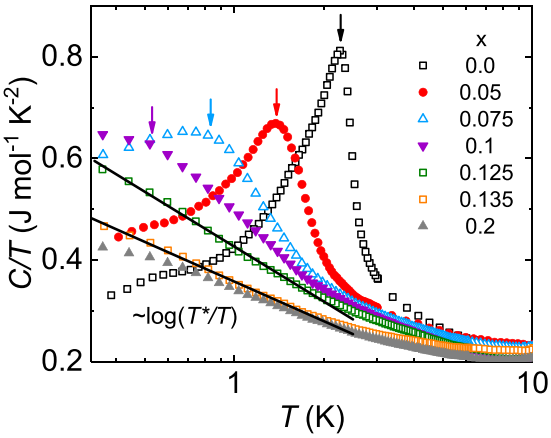

FIG. 4. Temperature dependence of the specific heat as C/T for $x \leqslant 0.2$. The arrows mark the position of the Curie temperature T_C. The black solid lines correspond to the $\ln(T^*/T)$ divergence of C/T.

to the ferromagnetic transition, where T_C gradually shifts to lower temperature with increasing x, and no transition is detected for $x \geqslant 0.125$, being consistent with $\rho(T)$ (Fig. 3). A logarithmic temperature dependence of C/T is also observed for $x = 0.125$ and 0.135, indicating the existence of strong quantum fluctuations for these concentrations, as observed at the FM QCP in stoichiometric $CeRh_6Ge_4$ [13]. In the paramagnetic state beyond $x = 0.135$, the divergent behavior of C/T is gradually suppressed upon further increasing x, which likely indicates the weakening of these fluctuations.

The temperature dependence of the magnetic susceptibility $\chi(T)$ and the magnetization as a function of field $M(H)$ at 0.5 K of $CeRh_6(Ge_{1-x}Si_x)_4$ are displayed in Fig. 5. For both $x = 0.05$ and 0.075, $\chi(T)$ shows a sharp increase upon cooling through the ferromagnetic transition, in line with that for stoichiometric $CeRh_6Ge_4$ [13], while there is only a small gradual increase for $x = 0.125$. As shown in Fig. 5(b), the magnetization loops at 0.5 K for $x \leqslant 0.075$ show clear hysteresis with a zero-field remanent magnetization, which are typical for FM order, suggesting that the nature of the magnetically ordered state does not change upon doping. Furthermore, also taking into account the stoichiometric case [13], the saturation moment at 0.5 K also decreases with increasing x, pointing to a corresponding decrease of the ordered moment. No ferromagnetic loop or hysteresis are observed in $M(H)$ for $x = 0.125$, suggesting a lack of FM order at 0.5 K.

Based on the measurements of the specific heat, resistivity, and susceptibility of $CeRh_6(Ge_{1-x}Si_x)_4$, the $T - x$ phase diagram is summarized in Fig. 6(a). The values of T_C obtained from C/T, $\rho(T)$, and $\chi(T)$ are all consistent, where T_C is continuously suppressed with increasing x before being no longer observed beyond $x_c = 0.125$. The evolution of magnetism upon silicon doping is similar to the $T - P$ phase diagram in stoichiometric $CeRh_6Ge_4$ [13], where T_C is linearly suppressed under pressure. As highlighted by the dashed line in Fig. 6(a), a critical concentration $x_c \approx 0.125$ can be obtained from a linear extrapolation of the slope of $T_C(x)$. $T_{\min}$ is determined from the minimum of $\rho(T)$, below which there is a $-\ln T$ dependence (see below), and this behavior abruptly

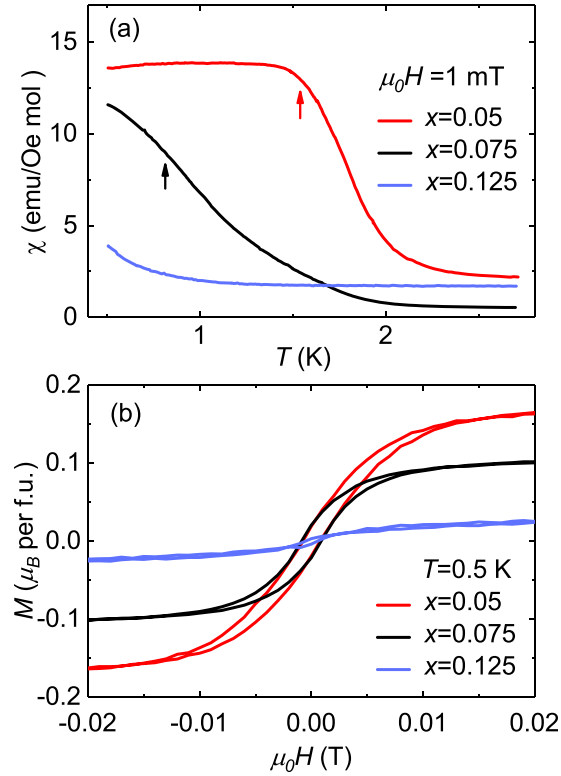

FIG. 5. (a) Temperature dependence of the magnetic susceptibility $\chi(T)$ for three compositions measured down to 0.5 K, in an applied field of 1 mT. The arrows mark the ferromagnetic transition at T_C corresponding to the inflection points. (b) Isothermal magnetization $M(H)$ as a function of field at 0.5 K for the three compositions.

appears for $x \geqslant 0.135$ and is almost independent of x at higher concentrations.

IV. DISCUSSION

The T_C of $CeRh_6(Ge_{1-x}Si_x)_4$ is continuously suppressed upon silicon doping, until it is no longer observed at a critical concentration of $x_c \approx 0.125$. Since the effect of isoelectronic silicon doping is primarily a pressure effect, this suggests that the mechanism for the suppression of T_C is similar to that observed for hydrostatic pressure, where a ferromagnetic quantum critical point and strange metal behavior is observed [13]. In order to compare the effects of chemical and hydrostatic pressures in $CeRh_6Ge_4$, the $T - P$ phase diagrams of $CeRh_6(Ge_{1-x}Si_x)_4$ and $CeRh_6Ge_4$ under pressure are summarized in Fig. 6(b). The evolution of T_C with chemical pressure P_{chem} for $CeRh_6(Ge_{1-x}Si_x)_4$ was derived from the inset of Fig. 1(d) and Fig. 6(a), and the evolution of T_C with pressure for stoichiometric $CeRh_6Ge_4$ is from Ref. [13]. All the T_C are continuously suppressed with increasing pressure P, indicating that the chemical pressure induced by silicon doping indeed has a similar effect to hydrostatic pressure on $CeRh_6Ge_4$. The difference between the data derived from applying hydrostatic and chemical pressure may be due to the pressure for the XRD measurements being measured at room temperature, while the pressure for transport measurements was determined at low temperatures.

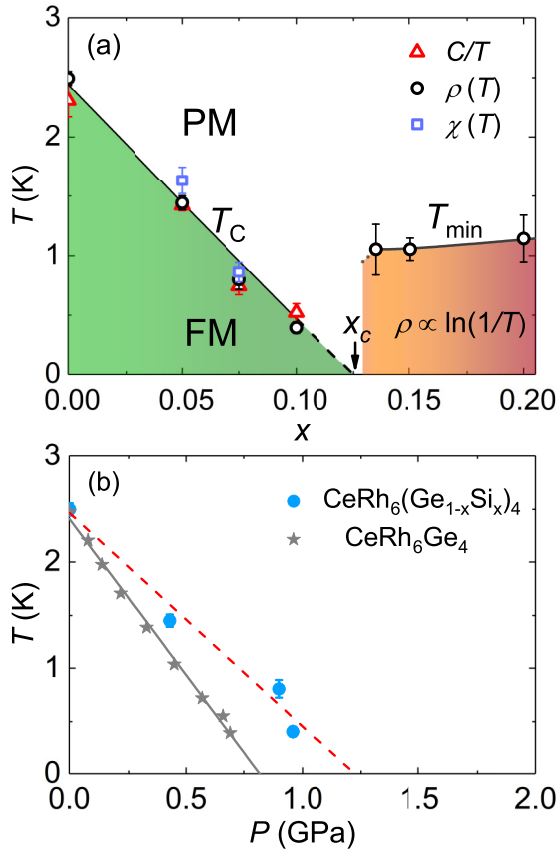

FIG. 6. (a) $T - x$ phase diagram of $CeRh_6(Ge_{1-x}Si_x)_4$. The triangles, circles, and squares represent T_C derived from the specific heat, resistivity, and magnetic susceptibility, respectively, and the errors correspond to the scattering of the low-T data. T_{min} denotes the onset of the low-temperature upturn in $\rho(T)$. (b) $T - P_{chem}$ phase diagram for $CeRh_6(Ge_{1-x}Si_x)_4$ and $T - P$ phase diagram for pressurized $CeRh_6Ge_4$. The evolution of T_C with pressure for stoichiometric $CeRh_6Ge_4$ is obtained from Ref. [13].

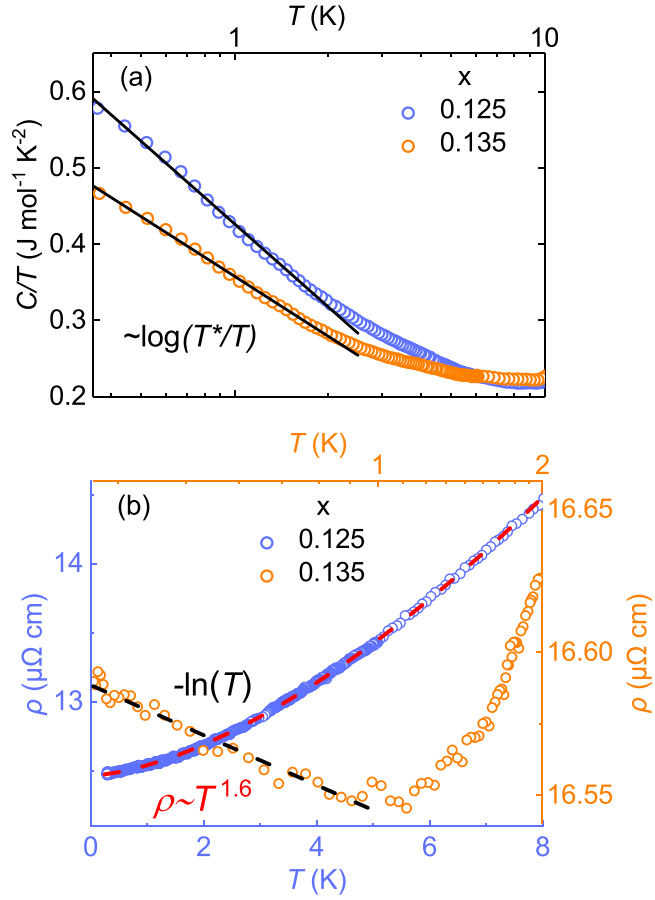

FIG. 7. (a) Temperature dependence of C/T for $x = 0.125$ and 0.135. The black solid lines correspond to the $\ln(T^*/T)$ divergence of C/T. (b) $\rho(T)$ for $x = 0.125$ and 0.135. The red dashed line corresponds to a fit with $\rho \propto T^{1.6}$, and the black dashed line represents a fit to $\rho(T) \propto -\ln T$.

As displayed in Fig. 7(a), a logarithmic temperature dependence of C/T is observed for $x = 0.125$ and 0.135, indicating the existence of strong quantum fluctuations in the vicinity of x_c. The concentration dependence of T_C and logarithmic divergence of C/T provide evidence for the existence of a FM QCP at $x_c \approx 0.125$. Such specific-heat behavior with $C/T \propto \ln(T^*/T)$ has been observed at the pressure-induced FM QCP of $CeRh_6Ge_4$ [13] as well as in La-doped $CeRh_6Ge_4$ [31]. However, while T-linear behavior of $\rho(T)$ is observed in pressurized stoichiometric $CeRh_6Ge_4$ at the FM QCP, it is not found in $CeRh_6(Ge_{1-x}Si_x)_4$ upon the suppression of FM order. As seen in Fig. 7(b), a $T^{1.6}$ dependence of $\rho(T)$ is observed at $x = 0.125$, while at a slightly higher concentration of $x = 0.135$, a low-temperature upturn with $\rho \sim -\ln(T)$ behavior occurs below T_{min}. The non-Fermi-liquid behavior with $T^{1.6}$ might arise from the interplay of disorder and spin fluctuations near a QCP as predicted for antiferromagnetic systems [32], where the resistivity varies as T^α with $1 \leqslant \alpha \leqslant 1.5$, depending on the degree of disorder. The $\rho \sim -\ln(T)$ observed for high-doping concentration samples in Si-doped $CeRh_6Ge_4$ is different from the $\rho = -AT$ reported in La-doped $CeRh_6Ge_4$ [31], which can be described in terms of a disordered Kondo model [2]. The low-temperature upturn for $x > 0.125$ may arise due to the moments not being fully screened by the Kondo effect, as observed for both some $5f$ electron compounds with $S > \frac{1}{2}$ [33,34], as well as some effective $S = \frac{1}{2}$ systems [35–37]. The $-\ln(T)$ behavior is characteristic of single-ion Kondo scattering, suggesting that there is predominantly incoherent Kondo scattering of the conduction electrons from the ground-state doublet. Additional studies are necessary to reveal the origin of the behaviors near x_c, as well as to determine the role played by disorder on the quantum critical behaviors and to directly confirm the presence of quantum criticality in $CeRh_6(Ge_{1-x}Si_x)_4$.

V. SUMMARY

In conclusion, we report an investigation of silicon substitution on the quantum critical ferromagnet $CeRh_6Ge_4$. The suppression of the Curie temperature T_C upon silicon doping and logarithmic divergence of C/T suggest the possible presence of a QCP at $x_c \approx 0.125$. Here the reduction of T_C with isoelectronic substitution of Si for Ge is attributed to the chemical pressure effect, where both hydrostatic and

chemical pressures reduce the unit-cell volume. At $x_c \approx 0.125$, a $\ln(T^*/T)$ behavior is observed in C/T, which is similar to the case of stoichiometric $CeRh_6Ge_4$ under pressure [13], but the resistivity deviates from the T-linear behavior observed for the stoichiometric compound, indicating the influence of disorder. In future, thermal expansion and neutron scattering are necessary to characterize the nature of the potential quantum criticality in $CeRh_6(Ge_{1-x}Si_x)_4$.

ACKNOWLEDGMENTS

This work was supported by the National Natural Science Foundation of China (Grants No. 12034017, No. 11974306, and No. 12174332), the National Key R&D Program of China (Grant No. 2017YFA0303100), the Key R&D Program of Zhejiang Province, China (Grant No. 2021C01002), and the Hubei Provincial Natural Science Foundation of China with Grant No. 2021CFB220.

[1] C. Pfleiderer, Superconducting phases of f-electron compounds, Rev. Mod. Phys. **81**, 1551 (2009).

[2] G. R. Stewart, Non-fermi-liquid behavior in d- and f -electron metals, Rev. Mod. Phys. **73**, 797 (2001).

[3] Z. F. Weng, M. Smidman, L. Jiao, X. Lu, and H. Q. Yuan, Multiple quantum phase transitions and superconductivity in Ce-based heavy fermions, Rep. Prog. Phys. **79**, 094503 (2016).

[4] M. A. Ruderman and C. Kittel, Indirect exchange coupling of nuclear magnetic moments by conduction electrons, Phys. Rev. **96**, 99 (1954).

[5] T. Kasuya, A theory of metallic ferro- and antiferromagnetism on Zener's model, Prog. Theor. Phys. **16**, 45 (1956).

[6] K. Yosida, Magnetic properties of Cu-Mn alloys, Phys. Rev. **106**, 893 (1957).

[7] S. Doniach, The Kondo lattice and weak antiferromagnetism, Phys. B+C (Amsterdam) **91**, 231 (1977).

[8] N. D. Mathur, F. M. Grosche, S. R. Julian, I. R. Walker, D. M. Freye, R. K. W. Haselwimmer, and G. G. Lonzarich, Magnetically mediated superconductivity in heavy fermion compound, Nature (London) **394**, 39 (1998).

[9] R. Küchler, N. Oeschler, P. Gegenwart, T. Cichorek, K. Neumaier, O. Tegus, C. Geibel, J. A. Mydosh, F. Steglich, L. Zhu, and Q. Si, Divergence of the Grüneisen Ratio at Quantum Critical Points in Heavy Fermion Metals, Phys. Rev. Lett. **91**, 066405 (2003).

[10] J. Custers, P. Gegenwart, H. Wilhelm, K. Neumaier, Y. Tokiwa, O. Trovarelli, C. Geibel, F. Steglich, C. Pepin, and P. Coleman, The break-up of heavy electrons at a quantum critical point, Nature (London) **424**, 524 (2003).

[11] H. V. Löhneysen, T. Pietrus, G. Portisch, H. G. Schlager, A. Schröder, M. Sieck, and T. Trappmann, Non-Fermi-Liquid Behavior in a Heavy-Fermion Alloy at a Magnetic Instability, Phys. Rev. Lett. **72**, 3262 (1994).

[12] M. Brando, D. Belitz, F. M. Grosche, and T. R. Kirkpatrick, Metallic quantum ferromagnets, Rev. Mod. Phys. **88**, 025006 (2016).

[13] B. Shen, Y. Zhang, Y. Komijani, M. Nicklas, R. Borth, A. Wang, Y. Chen, Z. Nie, R. Li, X. Lu, H. Lee, M. Smidman, F. Steglich, P. Coleman, and H. Yuan, Strange-metal behaviour in a pure ferromagnetic Kondo lattice, Nature (London) **579**, 51 (2020).

[14] H. Kotegawa, E. Matsuoka, T. Uga, M. Takemura, M. Manago, N. Chikuchi, H. Sugawara, H. Tou, and H. Harima, Indication of ferromagnetic quantum critical point in Kondo lattice $CeRh_6Ge_4$, J. Phys. Soc. Jpn. **88**, 093702 (2019).

[15] D. Belitz, T. R. Kirkpatrick, and T. Vojta, First Order Transitions and Multicritical Points in Weak Itinerant Ferromagnets, Phys. Rev. Lett. **82**, 4707 (1999).

[16] A. V. Chubukov, C. Pépin, and J. Rech, Instability of the Quantum-Critical Point of Itinerant Ferromagnets, Phys. Rev. Lett. **92**, 147003 (2004).

[17] A. Wang, F. Du, Y. Zhang, D. Graf, B. Shen, Y. Chen, Y. Liu, M. Smidman, C. Cao, F. Steglich, and H. Yuan, Localized 4f-electrons in the quantum critical heavy-fermion ferromagnet $CeRh_6Ge_4$, Sci. Bull. **66**, 1389 (2021).

[18] Y. Wu, Y. Zhang, F. Du, B. Shen, H. Zheng, Y. Fang, M. Smidman, C. Cao, F. Steglich, H. Yuan, J. D. Denlinger, and Y. Liu, Anisotropic $c-f$ Hybridization in the Ferromagnetic Quantum Critical Metal $CeRh_6Ge_4$, Phys. Rev. Lett. **126**, 216406 (2021).

[19] Y. H. Pei, Y. J. Zhang, Z. X. Wei, Y. X. Chen, K. Hu, Y.-F. Yang, H. Q. Yuan, and J. Qi, Unveiling the hybridization process in a quantum critical ferromagnet by ultrafast optical spectroscopy, Phys. Rev. B **103**, L180409 (2021).

[20] J. W. Shu, D. T. Adroja, A. D. Hillier, Y. J. Zhang, Y. X. Chen, B. Shen, F. Orlandi, H. C. Walker, Y. Liu, C. Cao, F. Steglich, H. Q. Yuan, and M. Smidman, Magnetic order and crystalline electric field excitations of the quantum critical heavy-fermion ferromagnet $CeRh_6Ge_4$, Phys. Rev. B **104**, L140411 (2021).

[21] L. Zhu, M. Garst, A. Rosch, and Q. Si, Universally Diverging Grüneisen Parameter and the Magnetocaloric Effect Close to Quantum Critical Points, Phys. Rev. Lett. **91**, 066404 (2003).

[22] A. Steppke, R. Küchler, S. Lausberg, E. Lengyel, L. Steinke, R. Borth, T. Lühmann, C. Krellner, M. Nicklas, C. Geibel, F. Steglich, and M. Brando, Ferromagnetic quantum critical point in the heavy-fermion metal $YbNi_4(P_{1-x}As_x)_2$, Science **339**, 933 (2013).

[23] A. Schröder, G. Aeppli, M. Adams, O. Stockert, H. V. Löhneysen, E. Bucher, R. Ramazashvili, and P. Coleman, Onset of antiferromagnetism in heavy-fermion metals, Nature (London) **407**, 351 (2000).

[24] Y. Sang, D. Belitz, and T. R. Kirkpatrick, Disorder Dependence of the Ferromagnetic Quantum Phase Transition, Phys. Rev. Lett. **113**, 207201 (2014).

[25] S. Ubaid-Kassis, T. Vojta, and A. Schroeder, Quantum Griffiths Phase in the Weak Itinerant Ferromagnetic Alloy $Ni_{1-x}\mathbf{V}_x$, Phys. Rev. Lett. **104**, 066402 (2010).

[26] T. Westerkamp, M. Deppe, R. Küchler, M. Brando, C. Geibel, P. Gegenwart, A. P. Pikul, and F. Steglich, Kondo-Cluster-Glass State near a Ferromagnetic Quantum Phase Transition, Phys. Rev. Lett. **102**, 206404 (2009).

[27] A. P. Pikul and D. Kaczorowski, Search for quantum criticality in a ferromagnetic system $UNi_{1-x}Co_xSi_2$, Phys. Rev. B **85**, 045113 (2012).

[28] E. Matsuoka, C. Hondo, T. Fujii, A. Oshima, H. Sugawara, T. Sakurai, H. Ohta, F. Kneidinger, L. Salamakha, H. Michor, and E. Bauer, Ferromagnetic transition at 2.5 K in the hexagonal Kondo-lattice compound $CeRh_6Ge_4$, J. Phys. Soc. Jpn. **84**, 073704 (2015).

[29] D. Voßwinkel, O. Niehaus, U. C. Rodewald, and R. Pöttgen, Bismuth flux growth of $CeRh_6Ge_4$ and $CeRh_2Ge_2$ single crystals, Z. Naturforsch. B **67**, 1241 (2012).

[30] F. Birch, Finite elastic strain of cubic crystals, Phys. Rev. **71**, 809 (1947).

[31] J.-C. Xu, H. Su, R. Kumar, S.-S. Luo, Z.-Y. Nie, A. Wang, F. Du, R. Li, M. Smidman, and H.-Q. Yuan, Ce-site dilution in the ferromagnetic Kondo lattice $CeRh_6Ge_4$, Chin. Phys. Lett. **38**, 087101 (2021).

[32] A. Rosch, Interplay of Disorder and Spin Fluctuations in the Resistivity near a Quantum Critical Point, Phys. Rev. Lett. **82**, 4280 (1999).

[33] V. H. Tran, J.-C. Griveau, R. Eloirdi, and E. Colineau, Ferromagnetic behavior of the Kondo lattice compound Np_2PtGa_3, Phys. Rev. B **89**, 054424 (2014).

[34] J. Schoenes, B. Frick, and O. Vogt, Transport properties of uranium monochalcogenide and monopnictide single crystals, Phys. Rev. B **30**, 6578 (1984).

[35] S. Nakatsuji, Y. Machida, Y. Maeno, T. Tayama, T. Sakakibara, J. van Duijn, L. Balicas, J. N. Millican, R. T. Macaluso, and Julia Y. Chan, Metallic Spin-Liquid Behavior of the Geometrically Frustrated Kondo Lattice $Pr_2Ir_2O_7$, Phys. Rev. Lett. **96**, 087204 (2006).

[36] Y. Luo, F. Ronning, N. Wakeham, X. Lu, T. Park, Z.-A. Xu, and J. D. Thompson, Pressure-tuned quantum criticality in the antiferromagnetic Kondo semimetal $CeNi_{2-\delta}As_2$, Proc. Natl. Acad. Sci. USA **112**, 13520 (2015).

[37] J. G. Sereni, T. Westerkamp, R. Küchler, N. Caroca-Canales, P. Gegenwart, and C. Geibel, Ferromagnetic quantum criticality in the alloy $CePd_{1-x}Rh_x$, Phys. Rev. B **75**, 024432 (2007).